

Does $H \rightarrow \gamma\gamma$ Taste Like Vanilla New Physics?

L. G. Almeida,^{1,*} E. Bertuzzo,^{1,†} P. A. N. Machado,^{1,2,‡} and R. Zukanovich Funchal^{1,2,§}

¹*Institut de Physique Théorique, CEA-Saclay, 91191 Gif-sur-Yvette, France*

²*Instituto de Física, Universidade de São Paulo, C. P. 66.318, 05315-970 São Paulo, Brazil*

We analyse the interplay between the Higgs to diphoton rate and electroweak precision measurements constraints in extensions of the Standard Model with new uncolored charged fermions that do not mix with the ordinary ones. We also compute the pair production cross sections for the lightest fermion and compare them with current bounds.

PACS numbers:

I. INTRODUCTION

The Standard Model (SM) has been so far exhaustively ratified by experiments. The recent discovery of a new boson, compatible with the SM Higgs particle, reported by ATLAS [1] and CMS [2] experiments at the Large Hadron Collider (LHC), finally inaugurates a new era in the field. For the first time we have access to the electroweak symmetry breaking sector of the SM and to the mysteries it may reveal.

Indeed, the combined analyses [3–5] of ATLAS and CMS results at 7 and 8 TeV [6–10] with the Tevatron experiments data [11] seem to suggest that physics beyond the SM is already here. There are two important facts that all these analyses seem to indicate: the gluon-gluon Higgs production cross section is $\sim 40\%$ smaller and the Higgs to diphoton decay ~ 3 larger than the SM prediction. Furthermore, the CMS uncombined Higgs data [2] clearly corroborate to this assessment. Their $H \rightarrow \gamma\gamma$ events tagged as produced by vector boson fusion prefer a production cross section ~ 2 times higher than the SM value, while their $H \rightarrow \gamma\gamma$ untagged events prefer it only $\sim 50\%$ higher. The former can be explained by an increase of $\Gamma(H \rightarrow \gamma\gamma)$ whereas the latter by an additional decrease of the gluon-gluon Higgs production cross section. Their $H \rightarrow ZZ$ events also point towards a $\sim 30\%$ lower gluon-gluon cross section.

In this paper we focus on the Higgs to diphoton decay as a possible smoking gun to new physics. The $H \rightarrow \gamma\gamma$ partial decay width, which appear only at loop level, is sensitive to the existence of extra charged states that couple to the Higgs boson. Such states arise in a variety of beyond the SM models. So since the first measurements by the LHC experiments suggested the observed Higgs to diphoton rate was larger than the SM one [12, 13], a number of works have studied the effect of new particles in this width [14–24].

We propose here to map, in a model independent way, which are the properties (masses, charges, couplings) that the new particles have to satisfy in order to account for the observed $H \rightarrow \gamma\gamma$ width in an economic way and pass the electroweak precision tests. We consider the effect of a single particle type at a time, in the smallest allowed $SU(2)_L \times U(1)_Y$ representations, assuming that possible additional states are sufficiently heavy to play no significant role. We also compute, in each case, their production cross section at the LHC and discuss possible signatures and limits.

This work is organized as follows. In the Sec. II we present the general framework of our approach to the $H \rightarrow \gamma\gamma$ width and in Sec. III we discuss the Doublet-Singlet and Triplet-Doublet uncolored fermion states, e.g. leptons, and their corresponding lagrangians we introduced in order to increase the diphoton rate. In Sec. IV we discuss what kind of enhancement are possible with these models and its dependency in the model parameters. In Sec. V we examine the constraints on the model parameters from the electroweak precision tests. In Sec. VI we consider the predictions for the pair production cross sections of these leptons states at the LHC operating at a center of mass energy of 8 TeV.

*Electronic address: leandro.almeida@cea.fr

†Electronic address: enrico.bertuzzo@cea.fr

‡Electronic address: accioly@fma.if.usp.br

§Electronic address: zukanov@if.usp.br

II. GENERAL FRAMEWORK

We assume the new 125 GeV particle observed at the LHC is in fact a SM-like Higgs boson, responsible for the electroweak symmetry breaking. It is a fundamental scalar transforming as part of the $SU(2)_L$ doublet

$$H = \begin{pmatrix} h^+ \\ h^0 \end{pmatrix}, \quad (1)$$

with the SM Higgs charge assignments and hypercharge $Y=1/2$.

The new particles will not mix with the SM fermions, they will only couple to the Higgs and the gauge sector respecting the SM symmetry group. This is feasible in a concrete model by having a new quantum number of an unbroken or nearly unbroken symmetry exclusive to the new sector. We will consider colorless fermion states in their lowest allowed $SU(2)_L \times U(1)_Y$ representations, *i.e.* singlets, doublets and triplets. Once the representation is chosen, their couplings with the SM gauge boson will be basically fixed. The only free parameters will be their couplings to the Higgs, their charges and their masses. We do not study here particles with $SU(3)_C$ quantum numbers, for simplicity and because we are not interested in this work to change the Higgs production cross section.

We will examine the allowed regions of these parameters in order for these new particles to significantly contribute to the Higgs diphoton width. We will do this by imposing $1.4 < \Gamma(H \rightarrow \gamma\gamma)/\Gamma^{\text{SM}}(H \rightarrow \gamma\gamma) < 5.4$ at 95% CL [3].

The Higgs to diphoton decay can be written in terms of the couplings to the particles in the loop as

$$\Gamma(H \rightarrow \gamma\gamma) = \frac{\alpha^2 m_H^3}{1024\pi^3} \left| \frac{2}{v} A_1(\tau_W) + \frac{8}{3v} A_{1/2}(\tau_t) + \frac{2g_{Hf\bar{f}}}{m_f} N_{c,f} q_f^2 A_{1/2}(\tau_f) + \frac{g_{HSS}}{m_S^2} N_{c,S} q_S^2 A_0(\tau_S) \right|^2, \quad (2)$$

where $\tau_a \equiv (m_H/2m_a)^2$, $a = W, t, f, S$, m_H is the Higgs mass, f (S) is a generic new fermion (scalar) with electric charge q_f (q_S), in units of the electric charge e , number of colors $N_{c,f}$ ($N_{c,S}$) and mass m_f (m_S), coupling to the Higgs with strength $g_{Hf\bar{f}}$ (g_{HSS}). The loop functions $A_1, A_{1/2}$ and A_0 are defined in the Appendix.

The first and second contributions are the usual SM ones, while the others are possible contributions from extra fermions and scalars. Since for the W boson contribution $A_1(\tau_W) \rightarrow -8.3$ and for the top quark $A_{1/2}(\tau_t) \rightarrow +1.8$, to increase $H \rightarrow \gamma\gamma$ we need to include a new negative contribution, at least as sizeable as the top one.

It was shown in Ref.[23], where the leading contributions from new particles to the diphoton decay width was derived from the QED beta functions, that for fermions carrying the same electric charge and described by the mass matrix M_f

$$\frac{2g_{Hf_i\bar{f}_i}}{m_{f_i}} = \frac{\partial}{\partial v} \log \lambda_{f_i}^2(v), \quad (3)$$

where $\lambda_{f_i}^2(v)$ is an eigenvalue of $M_f^\dagger M_f$. Clearly if fermions cannot mix they will all contribute to the loop with the same sign of the top contribution and decrease the Higgs to diphoton width. So a required condition to enhance the diphoton coupling to the Higgs is to have mixture. In this case the off-diagonal elements can enter with a term carrying the same sign of the W contribution, cancelling the top and increasing the width.

However, any physics beyond the SM must face its tremendous success: fulfill the electroweak precision tests and evade direct detection bounds.

New states will inevitably contribute to the vacuum polarization amplitudes of the electroweak gauge bosons $\Pi_{ab}^{\mu\nu}(q^2) = -ig^{\mu\nu}\Pi_{ab}(q^2) + q^\mu q^\nu$ terms [25, 26]. These new physics effects can be parametrized by the so-called quantum oblique parameters S , T and U defined as [26]

$$\begin{aligned} \alpha(M_Z^2) S^{\text{NP}} &= \frac{4s_W^2 c_W^2}{M_Z^2} \left[\Pi_{ZZ}^{\text{NP}}(M_Z^2) - \Pi_{ZZ}^{\text{NP}}(0) - \Pi_{\gamma\gamma}^{\text{NP}}(M_Z^2) - \frac{c_W^2 - s_W^2}{c_W s_W} \Pi_{\gamma Z}^{\text{NP}}(M_Z^2) \right] \\ \alpha(M_Z^2) T^{\text{NP}} &= \frac{\Pi_{WW}^{\text{NP}}(0)}{M_W^2} - \frac{\Pi_{ZZ}^{\text{NP}}(0)}{M_Z^2} \\ \alpha(M_Z^2) U^{\text{NP}} &= 4s_W^2 \left[\frac{\Pi_{WW}^{\text{NP}}(M_W^2) - \Pi_{WW}^{\text{NP}}(0)}{M_W^2} - c_W^2 \left(\frac{\Pi_{ZZ}^{\text{NP}}(M_Z^2) - \Pi_{ZZ}^{\text{NP}}(0)}{M_Z^2} \right) \right. \\ &\quad \left. - 2s_W c_W \frac{\Pi_{\gamma Z}^{\text{NP}}(M_Z^2)}{M_Z^2} - s_W^2 \frac{\Pi_{\gamma\gamma}^{\text{NP}}(M_Z^2)}{M_Z^2} \right], \end{aligned} \quad (4)$$

where $s_W^2 = \sin^2 \theta_W = 1 - c_W^2 \equiv 1 - \frac{M_W^2}{M_Z^2}$, M_Z and M_W are, respectively, the Z boson and W boson masses. By comparing the measurable electroweak observables with the theory prediction one finds the fitted values [27]

$$\begin{aligned}\Delta S &= S - S_{\text{SM}} = 0.04 \pm 0.10 \\ \Delta T &= T - T_{\text{SM}} = 0.05 \pm 0.11 \\ \Delta U &= U - U_{\text{SM}} = 0.08 \pm 0.11\end{aligned}\tag{5}$$

for the reference Higgs and top masses $M_{H,\text{ref}} = 120$ GeV and $m_{t,\text{ref}} = 173$ GeV, with the associated correlation matrix

$$V = \begin{pmatrix} 1 & +0.89 \\ +0.89 & 1 \end{pmatrix}.\tag{6}$$

We will include these constraints in our models by minimizing the χ^2 function defined as

$$\chi^2 = \sum_{i,j} (X_i^{\text{NP}} - X_i)(\sigma^2_{i,j})^{-1}(X_j^{\text{NP}} - X_j),\tag{7}$$

where $X_i = \Delta S, \Delta T$, are the fitted values of the oblique parameters with their corresponding uncertainties σ_i defined in Eq.(5), $X_i^{\text{NP}} = S^{\text{NP}}, T^{\text{NP}}$ are the contributions from the extra states that we will be introduced in each model investigated and $\sigma_{i,j}^2 \equiv \sigma_i V_{ij} \sigma_j$. In this work we will not consider ΔU because we do not expect it to impose any extra constraint on the parameter space. We will allow the values of the parameters of our models to vary such that $\Delta\chi^2 = \chi_{\text{min}}^2 + 2.28(+5.99)$, which correspond to 68% (95%) CL in a two-parameter fit. Since the difference between $M_{H,\text{ref}}$ and the actual Higgs mass $M_H = 125$ GeV is rather small and the uncertainties in the fitted parameters large, we will not correct for the exact result of the Higgs contribution to the oblique parameters.

Finally, since the new lepton states couple to Z and γ they can be pair-produced at the LHC. We will examine, in each case, the production cross-section and comment of possible existing limits and perspectives. In order to calculate the production cross sections we have implemented our models in calcHEP [28].

III. NEW FERMION STATES

The existence of chiral 4th generation that couples to the Higgs boson is excluded by data, since heavy quarks would contribute to Higgs production increasing its rate by a factor ~ 9 and excluding the Higgs up to 600 GeV [29]. To avoid this problem our fermions will be vector-like. We will also assume that our fermions will have some new quantum number so that they do not mix with the SM ones. In this case, we need to introduce at least two extra fermion fields in order to be able to build a renormalizable coupling term with the SM Higgs field. We will examine here the two lowest dimension possibilities given in Tab. I.

	SU(2) _L		
Field	Doublet-singlet	Triplet-doublet	U(1) _Y
$\chi_{L,R}$	2	3	$\hat{y} = y - \frac{1}{2}$
$\psi_{L,R}$	1	2	y

TABLE I: Representations of the new fermions and their corresponding hypercharges for the two cases we consider in this work.

A. Doublet-Singlet Model

For this case the lagrangian describing the new fermion masses and couplings with the Higgs is

$$-\mathcal{L}_H^{2+1} = c \overline{\psi_R} H \chi_L + c \tilde{H} \overline{\chi_R} P_L \psi_L + m_1 \overline{\chi_R} P_L \chi_L + m_2 \overline{\psi_R} P_L \psi_L + \text{h.c.},\tag{8}$$

where $\tilde{H} = i\tau_2 H^*$, c is the Yukawa coupling to the Higgs, $P_{L,R} = \frac{1}{2}(1 \pm \gamma_5)$, $m_{1,2}$ are the vector-like χ, ψ masses not coming from the Higgs sector.

After the electroweak symmetry breaking the Higgs acquires a vacuum expectation value (vev) v and also gives a mass contribution to the new fermions. The final mass matrix is

$$M_{2+1} = (\bar{\chi}_R^u \bar{\psi}_R \bar{\chi}_R^d) \begin{pmatrix} m_1 & cv & 0 \\ cv & m_2 & 0 \\ 0 & 0 & m_1 \end{pmatrix} \begin{pmatrix} \chi_L^u \\ \psi_L \\ \chi_L^d \end{pmatrix}. \quad (9)$$

To diagonalize M_{2+1} we introduce the following transformations

$$\omega_{L,R} \equiv \begin{pmatrix} \omega_{L,R}^1 \\ \omega_{L,R}^2 \end{pmatrix} = U_{L,R}^\dagger \begin{pmatrix} \psi_{L,R}^u \\ \chi_{L,R} \end{pmatrix} \quad (10)$$

where $U_{L,R}$ are unitary matrices, so defining the three mass eigenstates: ω^1 , ω^2 and χ^d with masses

$$M_\omega^{1,2} = \frac{1}{2} \left[(m_1 + m_2) \mp \sqrt{(m_2 - m_1)^2 + 4c^2 v^2} \right] \quad \text{and} \quad M_\chi = m_1, \quad (11)$$

$M_\omega^1 < M_\chi < M_\omega^2$, for most of the parameter values.

The gauge interactions with the SM fields are described by the usual coupling with the SM fields

$$\mathcal{L}_1^{2+1} = i\bar{\psi}\gamma^\mu (\partial_\mu - ig'y B_\mu) \psi + i\bar{\chi}\gamma^\mu (\partial_\mu - ig W_\mu^a T^a - ig'\hat{y} B_\mu) \chi, \quad (12)$$

where $g' = e/c_W$, $g = e/s_W$ are the SM couplings. One can show that the neutral current lagrangian will be

$$\begin{aligned} \mathcal{L}_{\text{NC}}^{2+1} = & e(\hat{y} - \frac{1}{2}) \bar{\chi}^d \gamma_\mu \chi^d A^\mu + (-\hat{y}g' s_W - \frac{1}{2} g c_W) \bar{\chi}^d \gamma_\mu \chi^d Z^\mu \\ & + \bar{\omega} \left[U_L^\dagger \begin{pmatrix} -(\hat{y} + \frac{1}{2})g' s_W & 0 \\ 0 & \frac{g}{2} c_W - \hat{y}g' s_W \end{pmatrix} U_L P_L + (L \rightarrow R) \right] \gamma_\mu \omega Z^\mu \\ & + e(\hat{y} + \frac{1}{2}) \bar{\omega} \gamma_\mu \omega A^\mu, \end{aligned} \quad (13)$$

and the charged current one

$$\mathcal{L}_{\text{CC}}^{2+1} = \frac{g}{\sqrt{2}} \bar{\omega} \gamma^\mu \left[U_L^\dagger P_L + U_R^\dagger P_R \right] W_\mu^+ \chi^d + \text{h.c.} \quad (14)$$

B. Triplet-Doublet Model

We will consider the following mass lagrangian for the new states

$$-\mathcal{L}_{\text{mass}}^{3+2} = c(\bar{\psi}_R \chi_L H + \bar{\psi}_L \chi_R H) + m_1 \bar{\chi}_L \chi_R + m_2 \bar{\psi}_L \psi_R + \text{h.c.}, \quad (15)$$

where c is their coupling to the SM Higgs field and m_1 and m_2 their bare masses. This gives rise, after electroweak symmetry breaking to the following mass matrix

$$M_{3+2} = (\bar{\psi}_R^u \bar{\chi}_R^a \bar{\psi}_R^d \bar{\chi}_R^b \bar{\chi}_R^c) \begin{pmatrix} m_2 & cv & 0 & 0 & 0 \\ cv & m_1 & 0 & 0 & 0 \\ 0 & 0 & m_2 & -c\frac{v}{\sqrt{2}} & 0 \\ 0 & 0 & -c\frac{v}{\sqrt{2}} & m_1 & 0 \\ 0 & 0 & 0 & 0 & m_1 \end{pmatrix} \begin{pmatrix} \psi_L^u \\ \chi_L^a \\ \psi_L^d \\ \chi_L^b \\ \chi_L^c \end{pmatrix}. \quad (16)$$

To diagonalize M_{3+2} we introduce the following transformations

$$\omega_{L,R} \equiv \begin{pmatrix} \omega_{L,R}^1 \\ \omega_{L,R}^2 \end{pmatrix} = U_{L,R}^\dagger \begin{pmatrix} \psi_{L,R}^u \\ \chi_{L,R}^a \end{pmatrix} \quad \xi_{L,R} \equiv \begin{pmatrix} \xi_{L,R}^1 \\ \xi_{L,R}^2 \end{pmatrix} = V_{L,R}^\dagger \begin{pmatrix} \psi_{L,R}^d \\ \chi_{L,R}^b \end{pmatrix} \quad (17)$$

where $U_{L,R}, V_{L,R}$ are unitary matrices, so defining the five mass eigenstates: $\omega^1, \omega^2, \xi^1, \xi^2$ and $\chi = \chi^c$ with masses

$$M_{\omega^{1,2}}^1 = \frac{1}{2} \left[(m_1 + m_2) \mp \sqrt{(m_2 - m_1)^2 + 4c^2 v^2} \right] \quad M_{\xi^{1,2}}^1 = \frac{1}{2} \left[(m_1 + m_2) \mp \sqrt{(m_2 - m_1)^2 + 2c^2 v^2} \right] \quad (18)$$

$$M_{\chi} = m_1 \quad (19)$$

$M_{\omega}^1 < M_{\xi}^1 < M_{\chi} < M_{\omega}^2 < M_{\xi}^2$, for most of the parameter values.

The gauge interactions with the SM fields are described again in the usual way by

$$\mathcal{L}_I^{3+2} = i\bar{\psi}\gamma^\mu (\partial_\mu - ig W_\mu^a T^a - ig' y B_\mu) \psi + i\bar{\chi}\gamma^\mu (\partial_\mu - ig W_\mu^a T^a - ig' \hat{y} B_\mu) \chi, \quad (20)$$

giving rise to the neutral current lagrangian

$$\begin{aligned} \mathcal{L}_{\text{NC}}^{3+2} = & e(\hat{y} - 1) \bar{\chi}\gamma_\mu \chi A^\mu + (-g' \hat{y} s_W - g c_W) \bar{\chi}\gamma_\mu \chi Z^\mu \\ & + \bar{\omega} \left[U_L^\dagger \begin{pmatrix} \frac{g}{2} c_W - yg' s_W & 0 \\ 0 & g c_W - \hat{y} g' s_W \end{pmatrix} U_L P_L + (L \rightarrow R) \right] \gamma_\mu \omega Z^\mu \\ & + (\hat{y} + 1) e \bar{\omega}\gamma_\mu \omega A^\mu \\ & + \bar{\xi} \left[V_L^\dagger \begin{pmatrix} -\frac{g}{2} c_W - yg' s_W & 0 \\ 0 & -\hat{y} g' s_W \end{pmatrix} V_L P_L + (L \rightarrow R) \right] \gamma_\mu \xi Z^\mu \\ & + \hat{y} e \bar{\xi}\gamma_\mu \xi A^\mu, \end{aligned} \quad (21)$$

and the charged current lagrangian

$$\mathcal{L}_{\text{CC}}^{3+2} = g (\bar{\omega} \bar{\xi} \bar{\chi}) \gamma^\mu \left[\begin{pmatrix} 0_{2 \times 2} & W_\mu^+ U_L^\dagger V_L' & 0_{2 \times 1} \\ W_\mu^- V_L'^\dagger U_L & 0_{2 \times 2} & V_L^\dagger \widetilde{W}_\mu^{+T} \\ 0 & \widetilde{W}_\mu^- V_L & 0 \end{pmatrix} P_L + (L \rightarrow R) \right] \begin{pmatrix} \omega \\ \xi \\ \chi \end{pmatrix}, \quad (22)$$

where $0_{n \times m}$ is a $n \times m$ zero matrix and we define $\widetilde{W}_\mu^- \equiv (0 \quad W_\mu^-)$, $\widetilde{W}_\mu^+ \equiv (0 \quad W_\mu^+)$ and

$$V_L' = \frac{1}{\sqrt{2}} \begin{pmatrix} V_{11L} & V_{12L} \\ \sqrt{2} V_{21L} & \sqrt{2} V_{22L} \end{pmatrix}. \quad (23)$$

IV. $H \rightarrow \gamma\gamma$ WIDTH

We have studied the Higgs to diphoton width in the Doublet-Singlet model and in the Triplet-Doublet model. In both models the ratio

$$R_{\gamma\gamma} = \frac{\Gamma^{\text{NP}}(H \rightarrow \gamma\gamma)}{\Gamma^{\text{SM}}(H \rightarrow \gamma\gamma)}, \quad (24)$$

between the width of $H \rightarrow \gamma\gamma$ with extra states and the width of $H \rightarrow \gamma\gamma$ in the SM have the feature that fixing the lightest new fermion mass the largest enhancement will be achieved when $m_1 = m_2$. This is illustrated in Fig. 1. These plots also show the symmetry between m_1 and m_2 that can be also seen from Eqs. (11) and (18).

In Fig. 2 we show the allowed regions at 68%, 95% and 99% CL, according to Ref. [3], for the ratio $R_{\gamma\gamma}$ in the plane $(m_1 = m_2) \times c$ for the doublet-singlet model and for several ω charges. We also show some iso-lines corresponding to the mass for the lightest new particle, either M_ω^1 or M_ω^2 , depending on the parameter values. The region where $M_\omega^{1,2} \lesssim 100$ GeV is already excluded by LEP data [30]. As a reference we also display some iso-lines for fixed values of $R_{\gamma\gamma}$.

In the Doublet-Singlet model there is only one electric charge at play in the extra states contribution, so there is no sensitivity to the sign of the charge. However, as m_1, m_2 and c vary one can have a complete cancellation of their contribution to $H \rightarrow \gamma\gamma$, and for a small parameter region, even have a smaller $\Gamma(H \rightarrow \gamma\gamma)$ than the SM one. For this reason, we have two disconnected regions that are consistent with a fixed $R_{\gamma\gamma}$. On the top panel of Fig. 2 those two

regions are very close together and for the most part concentrated at $M_\omega \lesssim 100$ GeV. As we increase the absolute charge of ω we start to see these regions being pulled apart and away from $M_\omega \lesssim 100$ GeV (see middle panel of Fig. 2) until one of the regions disappear from the plot.

For a coupling to the Higgs of $\mathcal{O}(1)$, for $y = 1$ and $M_\omega > 100$ GeV there is compatibility only if the future LHC data show a decrease of $\Gamma(H \rightarrow \gamma\gamma)$ to a value about 25% higher than the SM one, *i.e.*, in the 99% CL allowed region by the current LHC data. For $y > 1$ there are solutions even inside the 68% CL, for M_ω that can be as high as a few hundred of GeV, well inside the LHC discovery reach.

In Fig. 3 we show the allowed regions at 68%, 95% and 99% CL, according to Ref. [3], for the ratio $R_{\gamma\gamma}$ in the plane $(m_1 = m_2) \times c$ for the triplet-doublet model and for several ω charges. We also show some iso-lines corresponding to the mass for the lightest new particle, either M_ω^1 or M_ξ^1 , depending on the parameter values. The region where $M_{\omega,\xi} \lesssim 100$ GeV is already excluded by LEP data [30]. As a reference we also display some iso-lines for fixed $R_{\gamma\gamma}$.

In the Triplet-Doublet model there are four states and two different electric charges at play, so different charge combinations will give rise to a more interesting behavior. As before, and for the same reasons explained above, we have two disconnected regions that are consistent with a fixed $R_{\gamma\gamma}$. However, as we increase the charges these regions swap places.

In the top panels of Fig. 3 where the charges are, respectively, -3 (left panel) and -2 (right panel) for ω and -4 (left panel) and -3 (right panel) for ξ , we see only one of those regions. In the middle panels where the charges are, respectively, -1 (left panel) and 0 (right panel) for ω and -2 (left panel) and -1 (right panel) for ξ , we can see both regions, although most of the second allowed region is forbidden by the LEP limit. As we increase the charges as we can see in the lower panels, where ω has charge 2 (left panel) and 1 (right panel) and ξ has charge 3 (left panel) and 2 (right panel), the two regions crossover and swap places. We do not show here the case $y = 1/2$ because it is almost exactly the same as the top panel of Fig. 2, since ω have charge 1 and ξ charge 0 in this case.

For a coupling to the Higgs of $\mathcal{O}(1)$, the compatibility region where there is a solution for $R_{\gamma\gamma}$ at 68% and 95% CL strongly depends on the y value. Again the lightest particle can be within the LHC discovery range.

V. OBLIQUE PARAMETERS S AND T

We now examine the contributions of these new states to the oblique parameters. In Fig. 4 we show the allowed regions at 68%, 95% and 99% CL for S (left panel) and T (right panel) for the Doublet-Singlet model with $y = 1$ to illustrate the S and T separate behavior. S has two preferred regions, reflecting the same degeneracy we have seen before for $R_{\gamma\gamma}$. T , for $c \lesssim 0.5$ allows for any values of $m_1 = m_2$, but as c increases lower values of $m_1 = m_2$ become forbidden. This is because T is sensitive to the mass splitting of the doublet and prefers thus smaller mixing.

In Fig. 5 we show the the allowed regions at 68%, 95% and 99% CL for S (left panel) and T (right panel) for the Triplet-Doublet model for $y = -5/2$ to illustrate the S and T separate behavior. Here the second S region becomes a thin strip, while for T the behavior is very similar to the Doublet-Singlet case.

Now we will combine S and T using the χ^2 function described in Eq. (7) of Sec. II allowing for correlations between S and T . In Fig. 6 we show the combined region allowed for the fit of S and T , correlated, for $y = 1$ and $m_1 = m_2$ (left panel) and for $c = y = 1$ (right panel) for the Double-Singlet case. When we compare this with with Fig. 4 we see that the T parameter pulls the combined allowed region down. The plot on the right also shows the correlation between m_1 and m_2 allowed by T . In Fig. 7 we show the combined region allowed for the fit of S and T , correlated, for $y = -5/2$ and $m_1 = m_2$ (left panel) and for $c = 1$ and $y = -5/2$ (right panel) for the Triplet-doublet case.

In Fig. 8 we see that for the case where $y = 1$ there is great tension between the region that is preferred by $R_{\gamma\gamma}$ and the region allowed by S and T parameters. This is expected because T prefers a region where there is a small breaking of $SU(2)_L$ while $R_{\gamma\gamma}$ is mostly enhanced for large mixing. The same general behavior can be observed in Fig. 9 for $y = -5/2$ in the Triplet-Doublet model, although in this case, the tension is alleviated.

VI. PRODUCTION AT THE LHC

These new charged states could be produced at the LHC and we have calculated the cross section for pair production of the lightest lepton in the Doublet-Singlet model, and correspondingly in the Triplet-Doublet model.

This was done for p-p collisions at the LHC running at a center of mass energy of 8 TeV, using CalcHEP [28] with CTEQ6L parton distribution functions for the proton and imposing the following cuts: $-2.1 < \eta < 2.1$ and $p_T > 40$ GeV for each lepton.

For both models, we pair produce the lightest lepton through the process, $p + p \rightarrow \omega_1 + \bar{\omega}_1$. The main channels are the Neutral Currents Z and γ exchange.

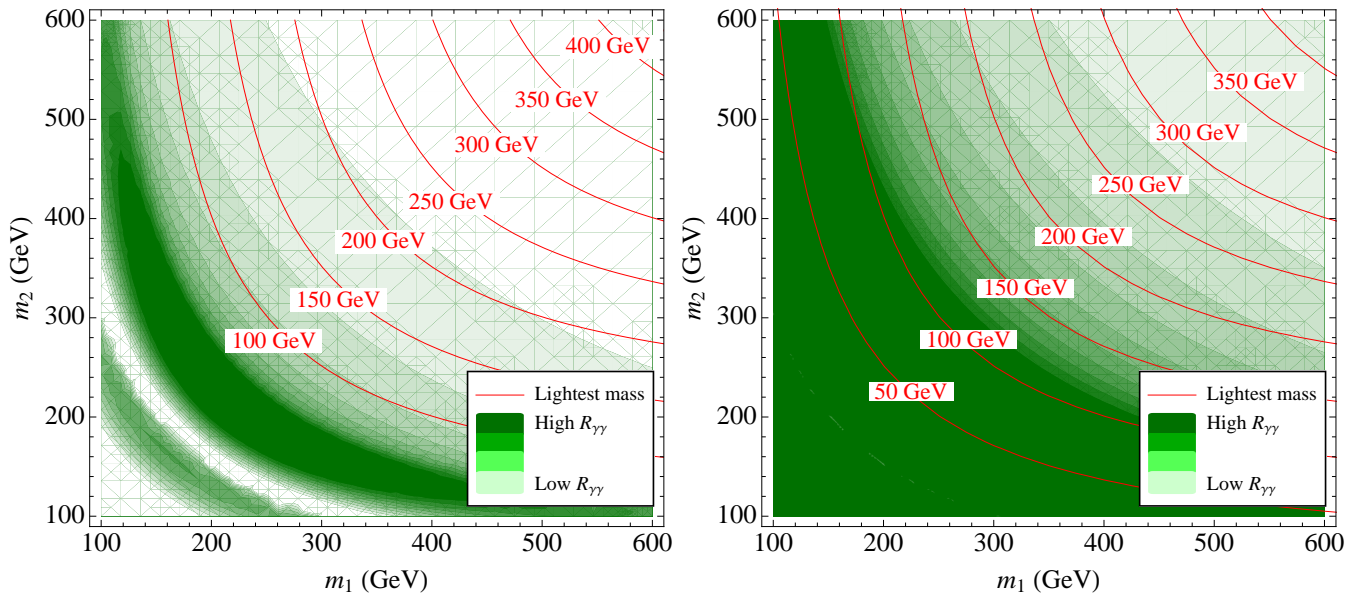


FIG. 1: Iso-contours of the ratio $R_{\gamma\gamma}$ in the plane m_1 versus m_2 for $c = 1$. We also show in the same plot the iso-lines that correspond to a fixed value of the lightest new charged fermion mass. The Doublet-Singlet model behaviour with $y = 1$ is illustrated on the left and the Triplet-Doublet model with $y = -5/2$ on the right panel.

In Fig. 10 the results of our calculations for the production cross section as a function of the mass of the lightest particle, for $y = 1$ for the Doublet-Singlet model and $y = -3/2$ for the Doublet-Triplet model. We also include in Fig. 10, the current bounds on the cross-section on stau from CMS [31].

These stringent bounds in the lower mass region could lead to some indication to the possible charges of these new leptons. For example, for masses > 300 GeV Figs. 2 and 3 point to a specific charges that preferred for the current allowed regions of $R_{\gamma\gamma}$. Additional structure to this sector, in the other hand, could permit one to evade them.

VII. CONCLUSIONS

We have investigated how the introduction of extra uncolored fermions, “leptons”, states which do not mix to the Standard Model fermions, but do couple to the Higgs, and therefore can affect the $H \rightarrow \gamma\gamma$ rate. We focus on the two smallest possibilities for the $SU(2)_L$ representation of the fermion fields that can give rise to a renormalizable lagrangian, coupling it to the Higgs, and contributing to the Higgs diphoton width: the doublet-singlet model and the triplet-double-model.

We map the masses, charges and couplings that these possible states must have in order to satisfy the current limits on $\Gamma(H \rightarrow \gamma\gamma)$ from the LHC and the Tevatron Higgs combined data [3] and confront them with the allowed ones from electroweak precision measurements.

We computed the pair production cross-section for the lightest states and compared it current bounds from long-lived charged particles.

Acknowledgments

This work was supported by Fundação de Amparo à Pesquisa do Estado de São Paulo (FAPESP), Conselho Nacional de Desenvolvimento Científico e Tecnológico (CNPq), by the European Commission under the contract PITN-GA-2009-237920 and by the Agence National de la Recherche under contract ANR 2010 BLANC 0413 01. We thank O.J.P. Éboli for useful comments and discussions.

Note added: During the finalization of this paper Ref. [32, 33] appeared.

Appendix: Definitions of Some Functions Used in this Work

Here we for completeness we define the loop functions used to compute $\Gamma(H \rightarrow \gamma\gamma)$.

$$A_1(\tau) = -[2\tau^2 + 3\tau + 3(2\tau - 1)g(\tau)]/\tau^2 \quad (25)$$

$$A_{1/2}(\tau) = 2[\tau + (\tau - 1)g(\tau)]/\tau^2 \quad (26)$$

$$A_0(\tau) = -[\tau - g(\tau)]/\tau^2 \quad (27)$$

where $g(\tau) = \arcsin^2 \sqrt{\tau}$, for $\tau \leq 1$.

For the fermion gauge boson interaction lagrangian that can be generically written as

$$\mathcal{L}_{Vf_i f_j} = \bar{f}_i (g_{LV}^{ij} P_L + g_{RV}^{ij} P_R) \gamma_\mu f_j V^\mu$$

we define the two point functions that enter in the oblique parameters calculation in terms of the generic couplings and of the universal functions $\Pi_{V\pm A}$ as [19, 34]

$$\Pi_{V_1 V_2}(s) = (g_{LV_1}^{ij} g_{LV_2}^{ij} + g_{RV_1}^{ij} g_{RV_2}^{ij}) \Pi_{V+A}(s, m_i, m_j) + (g_{LV_1}^{ij} g_{RV_2}^{ij} + g_{LV_2}^{ij} g_{RV_1}^{ij}) \Pi_{V-A}(s, m_i, m_j), \quad (28)$$

where $V_1, V_2 = W, Z, \gamma$, m_i and m_j are the masses of the fermions f_i and f_j in the loop and

$$\begin{aligned} \Pi_{V+A}(s, m_i, m_j) = & -\frac{N_c}{24\pi^2} \left[m_i^2 \ln m_i^2 \left(1 - \frac{(m_i^2 - m_j^2)}{2s} \right) + m_j^2 \ln m_j^2 \left(1 - \frac{(m_j^2 - m_i^2)}{2s} \right) - \frac{s}{3} + \frac{(m_i^2 - m_j^2)^2}{2s} \right. \\ & \left. + \left(s - \frac{(m_i^2 + m_j^2)}{2} - \frac{(m_i^2 - m_j^2)^2}{2s} \right) (\bar{B}_0(s, m_i, m_j) - \ln(m_i m_j)) + \Delta_{\text{div}} \right], \end{aligned} \quad (29)$$

and

$$\Pi_{V-A}(s, m_i, m_j) = -\frac{N_c}{8\pi^2} m_i m_j (\bar{B}_0(s, m_i, m_j) - \ln(m_i m_j) + \Delta_\epsilon), \quad (30)$$

here N_c are the number of colors, the divergent part $\Delta_{\text{div}} \equiv \Delta_\epsilon (s - \frac{3}{2}(m_i^2 + m_j^2))$ with $\Delta_\epsilon = \frac{2}{\epsilon} - \gamma + \ln 4\pi + \ln \mu^2$.

We have used the finite part of the B_0 function

$$\bar{B}_0(s, m_i, m_j) = 1 - \frac{m_i^2 + m_j^2}{m_i^2 - m_j^2} \ln\left(\frac{m_i}{m_j}\right) + F(s, m_i, m_j), \quad (31)$$

with

$$F(s, m_i, m_j) = -1 + \frac{m_i^2 + m_j^2}{m_i^2 - m_j^2} \ln\left(\frac{m_i}{m_j}\right) - \int_0^1 dx \ln \left(\frac{x^2 - x(s + m_i^2 - m_j^2) + m_i^2 - i\epsilon}{m_i m_j} \right). \quad (32)$$

as defined in Ref. [34].

-
- [1] ATLAS Collaboration, F. Gianotti, <http://indico.cern.ch/conferenceDisplay.py?confId=197461>.
 - [2] CMS Collaboration, J. Incandela, <http://indico.cern.ch/conferenceDisplay.py?confId=197461>.
 - [3] T. Corbett, O. J. P. Eboli, J. Gonzalez-Fraile and M. C. Gonzalez-Garcia, arXiv:1207.1344 [hep-ph].
 - [4] P. P. Giardino, K. Kannike, M. Raidal and A. Strumia, arXiv:1207.1347 [hep-ph].
 - [5] J. R. Espinosa, C. Grojean, M. Muhlleitner and M. Trott, arXiv:1207.1717 [hep-ph].
 - [6] ATLAS Collaboration, G. Aad *et al.*, (2012), arXiv:1207.0319.
 - [7] CMS Collaboration, S. Chatrchyan *et al.*, Phys.Lett. **B710**, 26 (2012), arXiv:1202.1488.
 - [8] CMS Collaboration, CMS PAS HIG-12-015.
 - [9] CMS Collaboration, CMS PAS HIG-12-020.
 - [10] ATLAS Collaboration, ATLAS-CONF-2012-091.

- [11] The CDF Collaboration, the D0 Collaboration, the Tevatron New Physics, Higgs Working Group, arXiv:1207.0449.
- [12] S. Chatrchyan *et al.* [CMS Collaboration], Phys. Lett. B **710**, 403 (2012) [arXiv:1202.1487 [hep-ex]].
- [13] G. Aad *et al.* [ATLAS Collaboration], Phys. Rev. Lett. **108**, 111803 (2012) [arXiv:1202.1414 [hep-ex]].
- [14] J. Cao, Z. Heng, T. Liu and J. M. Yang, Phys. Lett. B **703**, 462 (2011) [arXiv:1103.0631 [hep-ph]].
- [15] A. Alves, E. Ramirez Barreto, A. G. Dias, C. A. de S.Pires, F. S. Queiroz and P. S. Rodrigues da Silva, Phys. Rev. D **84**, 115004 (2011) [arXiv:1109.0238 [hep-ph]].
- [16] M. Carena, S. Gori, N. R. Shah and C. E. M. Wagner, JHEP **1203**, 014 (2012) [arXiv:1112.3336 [hep-ph]].
- [17] P. Draper and D. McKeen, Phys. Rev. D **85**, 115023 (2012) [arXiv:1204.1061 [hep-ph]].
- [18] K. Kumar, R. Vega-Morales and F. Yu, arXiv:1205.4244 [hep-ph].
- [19] S. Dawson and E. Furlan, arXiv:1205.4733 [hep-ph].
- [20] M. Carena, S. Gori, N. R. Shah, C. E. M. Wagner and L. -T. Wang, arXiv:1205.5842 [hep-ph].
- [21] A. G. Akeroyd and S. Moretti, arXiv:1206.0535 [hep-ph].
- [22] D. Carmi, A. Falkowski, E. Kuflik and T. Volansky, arXiv:1206.4201 [hep-ph].
- [23] M. Carena, I. Low and C. E. M. Wagner, arXiv:1206.1082 [hep-ph].
- [24] D. Carmi, A. Falkowski, E. Kuflik, T. Volansky and J. Zupan, arXiv:1207.1718 [hep-ph].
- [25] G. Altarelli and R. Barbieri, Phys. Lett. B **253**, 161 (1991).
- [26] M. E. Peskin and T. Takeuchi, Phys. Rev. D **46**, 381 (1992).
- [27] M. Baak, M. Goebel, J. Haller, A. Hoecker, D. Ludwig, K. Moenig, M. Schott and J. Stelzer, Eur. Phys. J. C **72**, 2003 (2012) [arXiv:1107.0975 [hep-ph]].
- [28] A. Pukhov, CalcHEP 2.3: MSSM, structure functions, event generation, batchs, and generation of matrix elements for other packages, arXiv:hep-ph/0412191.
- [29] CMS collaboration, PAS EXO-11-098
- [30] P. Achard *et al.* [L3 Collaboration], Phys. Lett. B **517**, 75 (2001) [hep-ex/0107015].
- [31] S. Chatrchyan *et al.* [CMS Collaboration], Phys. Lett. B **713**, 408 (2012) [arXiv:1205.0272 [hep-ex]].
- [32] A. Joglekar, P. Schwaller and C. E. M. Wagner, arXiv:1207.4235.
- [33] N. Arkani-Hamed, K. Blum, R. Tito D'Agnolo and J. Fan, arXiv:1207.4482.
- [34] W.F.L. Hollik, DESY 88-188.

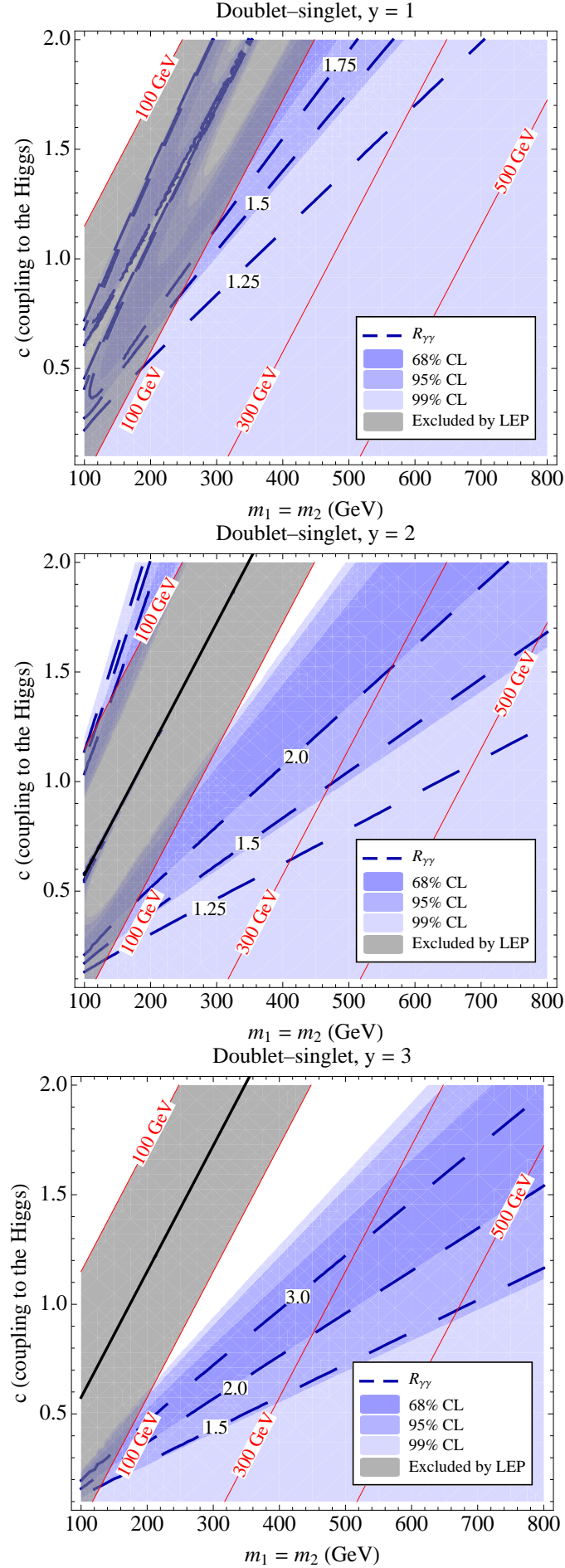


FIG. 2: Regions in the plane $(m_1 = m_2) \times c$ allowed by the fit to the combined Higgs data for $R_{\gamma\gamma}$, according to Ref. [3] at 68% (darker blue), 95% (intermediate blue) and 99% (lighter blue) CL, for the doublet-singlet model. We also show some iso-lines

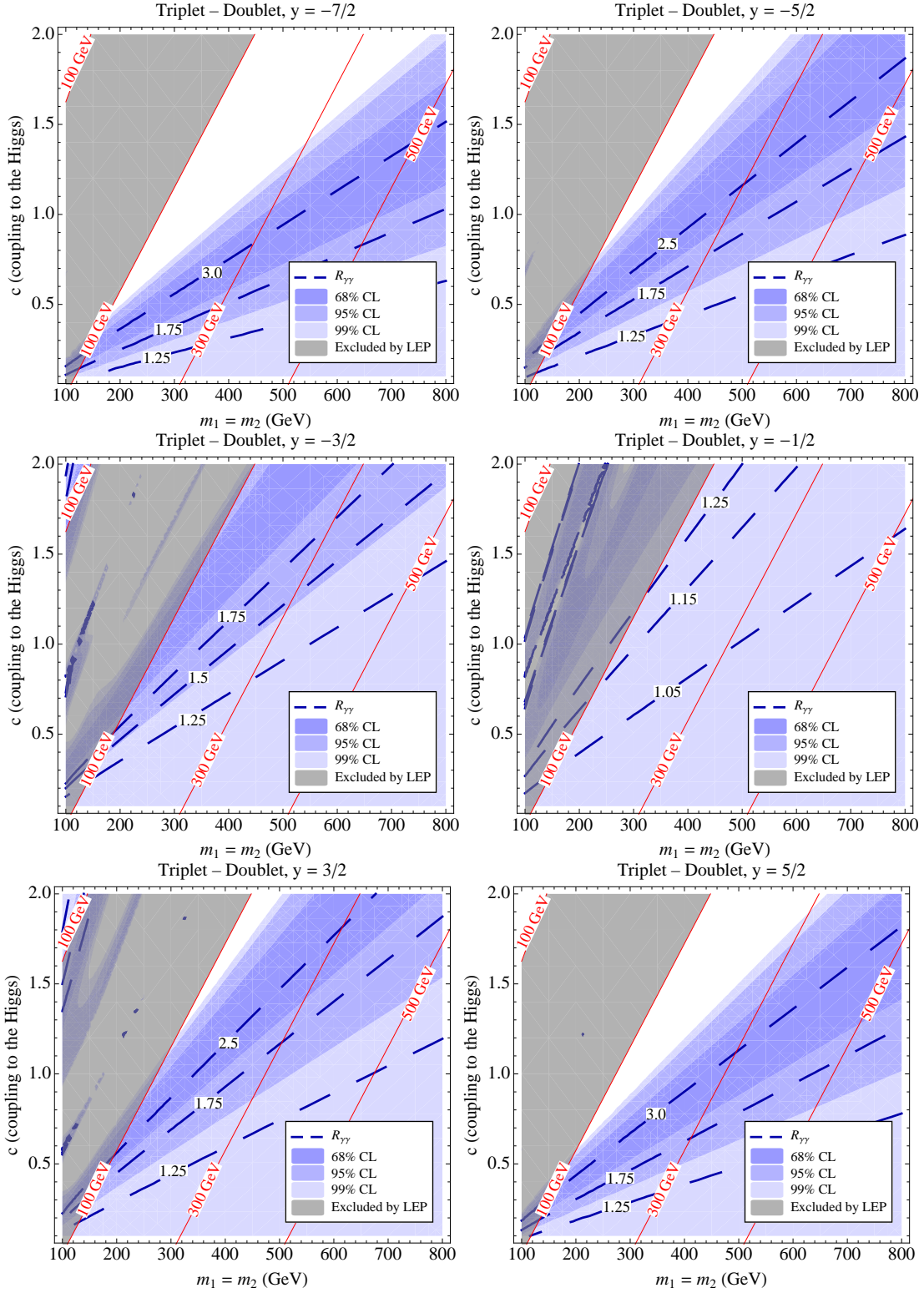


FIG. 3: Regions in the plane $(m_1 = m_2) \times c$ allowed by the fit to the combined Higgs data for $R_{\gamma\gamma}$, according to Ref. [3] at 68% (darker blue), 95% (intermediate blue) and 99% (lighter blue) CL, for the triplet-doublet model. We also show some iso-lines of constant mass for the lightest new particle, M_ω^1 or M_ξ^1 , depending on the parameter values. The region excluded by LEP, for M_ω^1 (or M_ξ^1) $\lesssim 100$ GeV, is shown in grey. As a reference we also show some isolines that correspond to $R_{\gamma\gamma} = 1.05, 1.15, 1.25, 1.5, 1.75$ and 2.5 . On the top panel we show on the left (right) the case $y = -7/2$ ($y = -5/2$) that correspond to ω and ξ with charges -3 and -4 (-2 and -3), respectively. On the middle panel we show on the left (right) the case $y = -3/2$ ($y = -1/2$) that correspond to ω and ξ with charges -1 and -2 (0 and -1), respectively. On the lower panel we show on the left (right) the case $y = 3/2$ ($y = 5/2$) that correspond to ω and ξ with charges 2 and 1 (3 and 2), respectively.

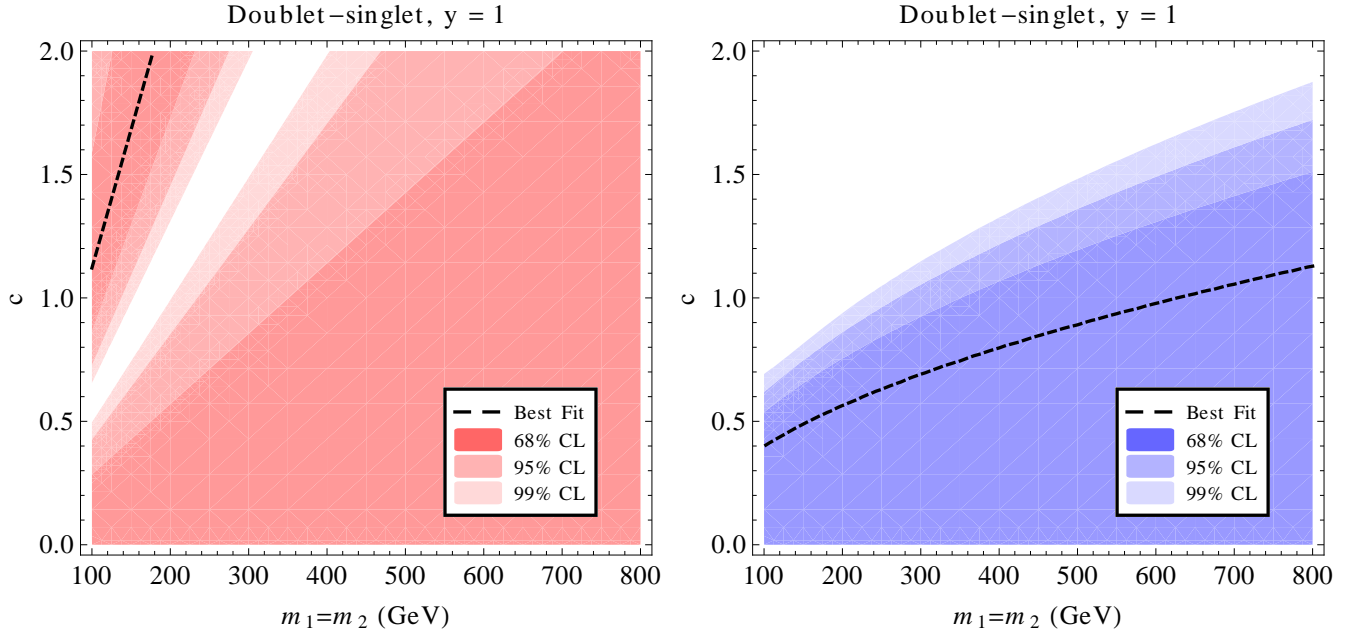


FIG. 4: Allowed regions for S (left panel) and T (right panel) in the plane $m_1 = m_2$ versus c , the coupling to the Higgs for the Doublet-singlet model with $y = 1$.

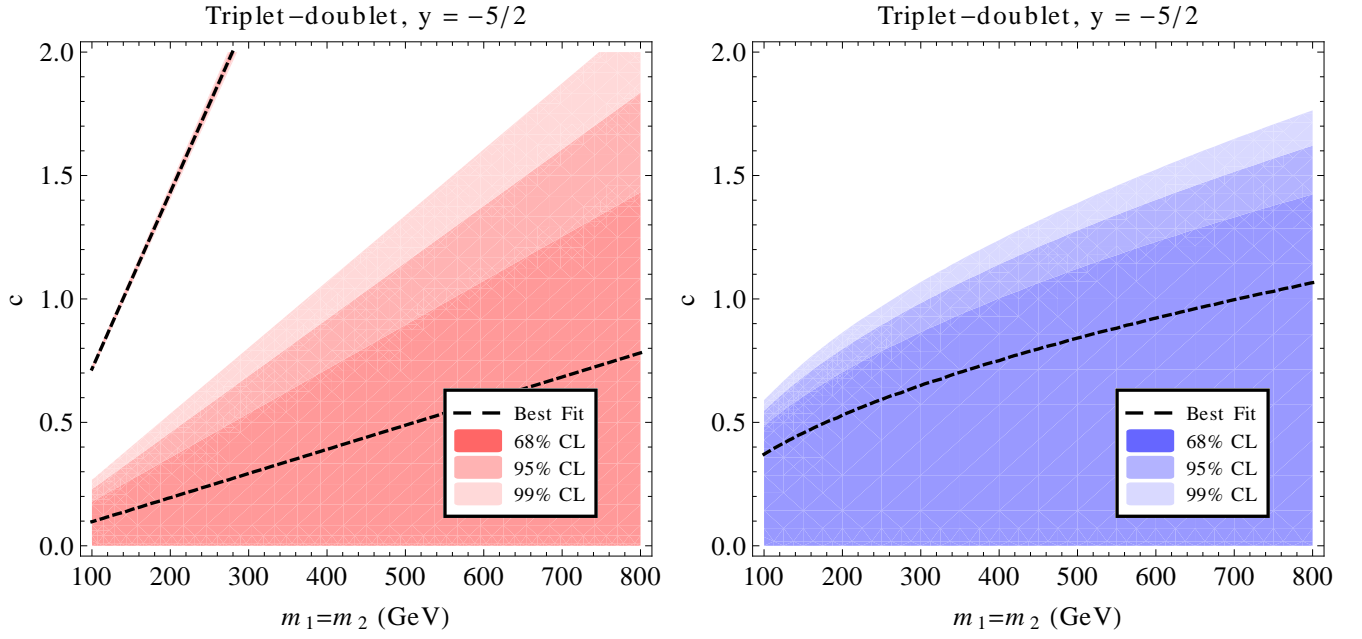


FIG. 5: Allowed regions for S (left panel) and T (right panel) in the plane $m_1 = m_2$ versus c , the coupling to the Higgs for the Triplet-doublet model with $y = -5/2$.

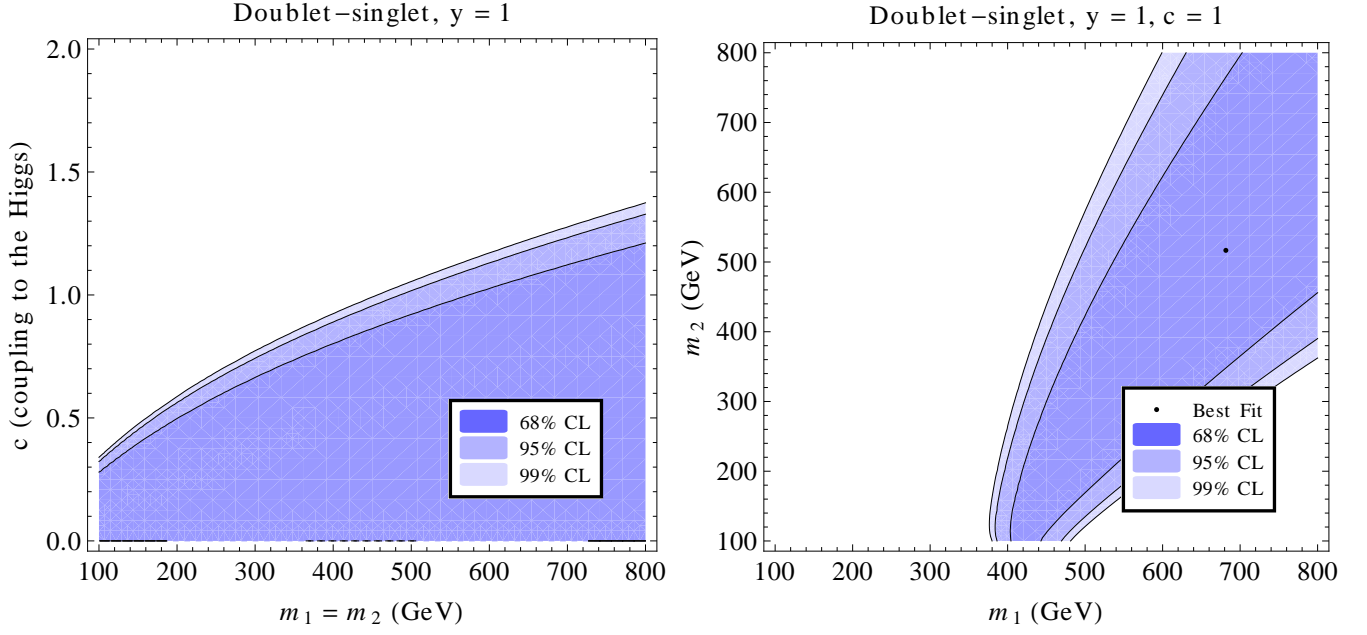


FIG. 6: Allowed region for the combined fit of S and T for $y = 1$ and $m_1 = m_2$ (left panel) and for $y = 1$ and $c = 1$ (right panel) in the Doublet-Singlet model.

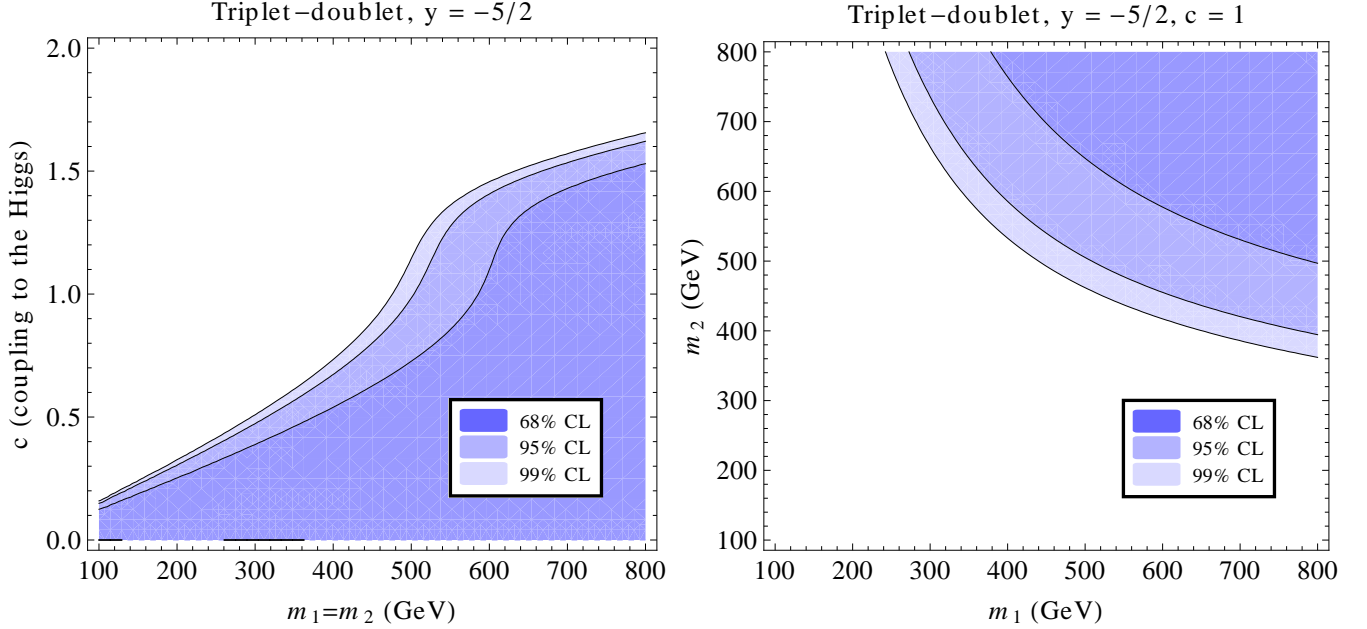


FIG. 7: Allowed region for the combined fit of S and T for $y = -5/2$ and $m_1 = m_2$ (left panel) and for $y = -5/2$ and $c = 1$ (right panel) in the Triplet-Doublet model.

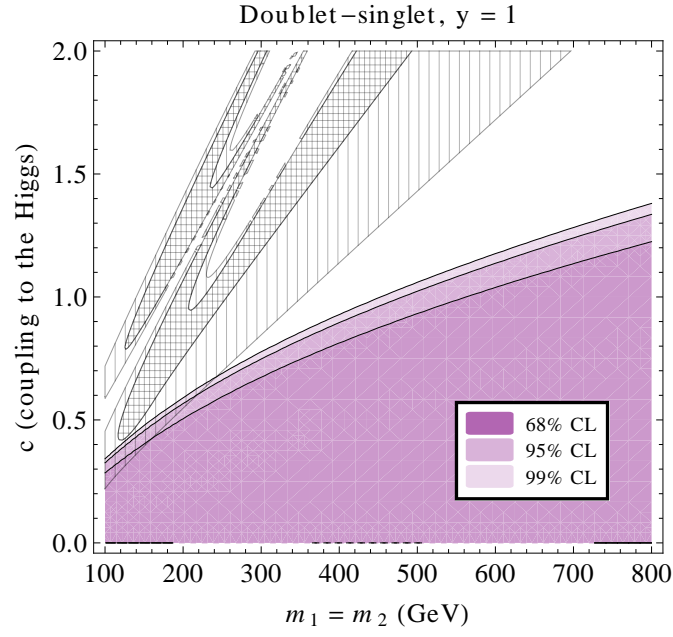


FIG. 8: Allowed region for the combined fit of S and T for $y = 1$ in the Doublet-Singlet model and its compatibility to $R_{\gamma\gamma}$. We show the $R_{\gamma\gamma}$ allowed regions at 68% and 95 % CL.

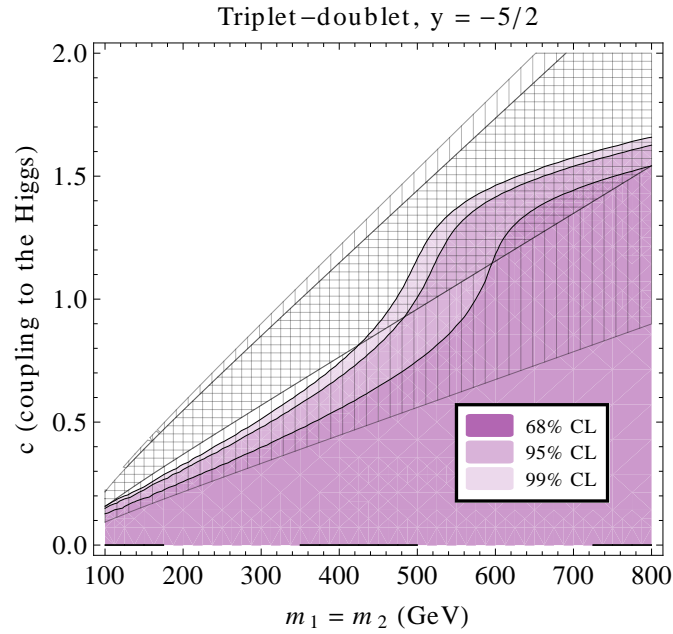


FIG. 9: Allowed region for the combined fit of S and T for $y = -5/2$ in the Triplet-Doublet model and its compatibility to $R_{\gamma\gamma}$. We show the $R_{\gamma\gamma}$ allowed regions at 68% and 95 % CL.

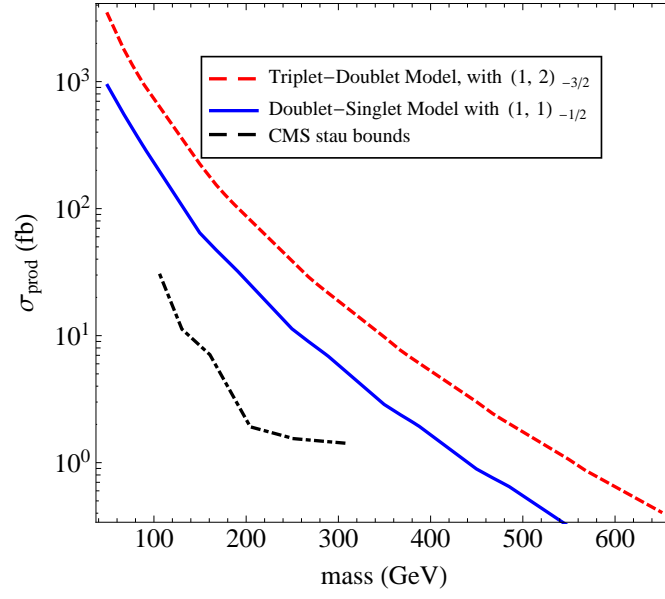


FIG. 10: Pair production cross section for the lightest new state in the Doublet-Singlet model with $y = 1$ and in the Triplet-Doublet model with $y = -5/2$. We also show the CMS limit for long lived staus pair production [31] at 7 TeV.